THEORETICAL MODELS FOR PREDICTING THE ACOUSTIC CHARACTERISTICS OF FIBRE-REINFORCED MATERIALS

E A Skelton*

Imperial College of Science, Technology & Medicine, London SW7 2BZ

1 INTRODUCTION

The use of fibre reinforced materials is becoming more common as they can be used to form strong lightweight structures. There is therefore a requirement to understand their acoustic properties. The theoretical methods outlined in this paper have been developed at Imperial College and at DRA Haslar to provide a basis for computer programs to predict numerically the acoustic scattering by, or radiation from, certain relevant canonical problems. Parametric studies using such programs should help to identify the physical mechanisms controlling the acoustic properties of these materials. Previous work at DRA has developed theoretical methods and computer programs for analyzing a variety of problems in which each component is isotropic. The aim of the current work was to extend these models so that they can include anisotropic components. The four models discussed in this paper are planar layered media [1], cylindrically layered media [2], a rib stiffened cylindrical shell [3] and a finite axisymmetric body [4]. The previous work makes use of the method of 'dynamic stiffness coupling in the spectral domain' to assemble elements of acoustic fluid, viscous fluid and isotropic elastic solids into a global system matrix equation, from which it is straightforward to obtain acoustic properties. This method will be used here also. Thus for planar layers in the $x-y$ plane, see Figure 1, spectral quantities are obtained by Fourier transformation with respect to x and y, e.g. for the displacement

$$\begin{pmatrix} \overline{u}_x(\alpha,\beta,z) \\ \overline{u}_y(\alpha,\beta,z) \\ \overline{u}_z(\alpha,\beta,z) \end{pmatrix} = \int_{-\infty}^{\infty}\int_{-\infty}^{\infty} \begin{pmatrix} u_x(x,y,z) \\ u_y(x,y,z) \\ u_z(x,y,z) \end{pmatrix} \mathrm{e}^{-\mathrm{i}\alpha x}\mathrm{e}^{-\mathrm{i}\beta y}\,\mathrm{d}x\mathrm{d}y \tag{1.1}$$

with the inverse

$$\begin{pmatrix} u_x(x,y,z) \\ u_y(x,y,z) \\ u_z(x,y,z) \end{pmatrix} = \frac{1}{(2\pi)^2}\int_{-\infty}^{\infty}\int_{-\infty}^{\infty} \begin{pmatrix} \overline{u}_x(\alpha,\beta,z) \\ \overline{u}_y(\alpha,\beta,z) \\ \overline{u}_z(\alpha,\beta,z) \end{pmatrix} \mathrm{e}^{\mathrm{i}\alpha x}\mathrm{e}^{\mathrm{i}\beta y}\,\mathrm{d}x\mathrm{d}y \tag{1.2}$$

whilst in cylindrical (r,ϕ,z) geometry, see Figure 2, it is natural to make use of Fourier transforms with respect to z and Fourier series with respect to ϕ:

$$\begin{pmatrix} \overline{u}_z(r,n,\alpha) \\ \overline{u}_\phi(r,n,\alpha) \\ \overline{u}_r(r,n,\alpha) \end{pmatrix} = \frac{1}{2\pi}\int_0^{2\pi}\int_{-\infty}^{\infty} \begin{pmatrix} u_z(r,\phi,z) \\ u_\phi(r,\phi,z) \\ u_r(r,\phi,z) \end{pmatrix} \mathrm{e}^{-\mathrm{i}n\phi}\mathrm{e}^{-\mathrm{i}\alpha z}\,\mathrm{d}z\mathrm{d}\phi \tag{1.3}$$

whose inverse is

$$\begin{pmatrix} u_z(r,\phi,z) \\ u_\phi(r,\phi,z) \\ u_r(r,\phi,z) \end{pmatrix} = \frac{1}{2\pi}\sum_{n=-\infty}^{\infty}\mathrm{e}^{\mathrm{i}n\phi}\int_{-\infty}^{\infty} \begin{pmatrix} \overline{u}_z(r,n,\alpha) \\ \overline{u}_\phi(r,n,\alpha) \\ \overline{u}_r(r,n,\alpha) \end{pmatrix} \mathrm{e}^{\mathrm{i}\alpha z}\,\mathrm{d}\alpha. \tag{1.4}$$

In these and all subsequent equations the time-harmonic factor $\exp(-\mathrm{i}\omega t)$ is omitted.

For the linear theories used in acoustics the surface spectral stresses at the layer boundaries can be linearly related to the displacements in each of the three coordinate directions there. Hence for the mth layer

$$\mathbf{S}^{(m)}\mathbf{u}^{(m)} = \hat{\boldsymbol{\sigma}}^{(m)} \tag{1.5}$$

where, see Figure 3, in the planar geometry

*The work described in this paper has been undertaken for DRA and has been carried out by E. A. Skelton at Imperial College and by J. H. James at DRA, Haslar, Gosport, Hants PO12 2AG.

THEORETICAL METHODS FOR FIBRE-REINFORCED MATERIALS

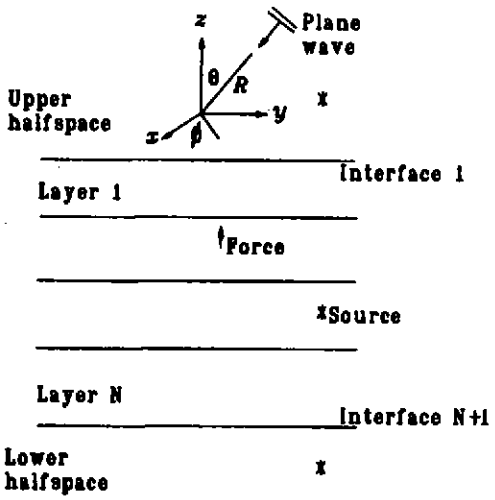

Figure 1: Geometry and Co-ordinate System for Planar Layers

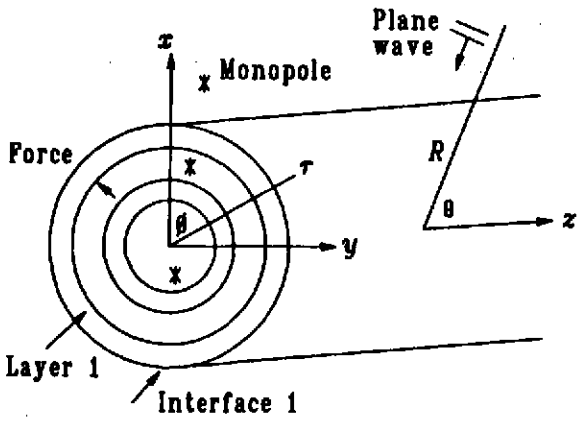

Figure 2: Geometry and Co-ordinate System for Cylindrical Layers

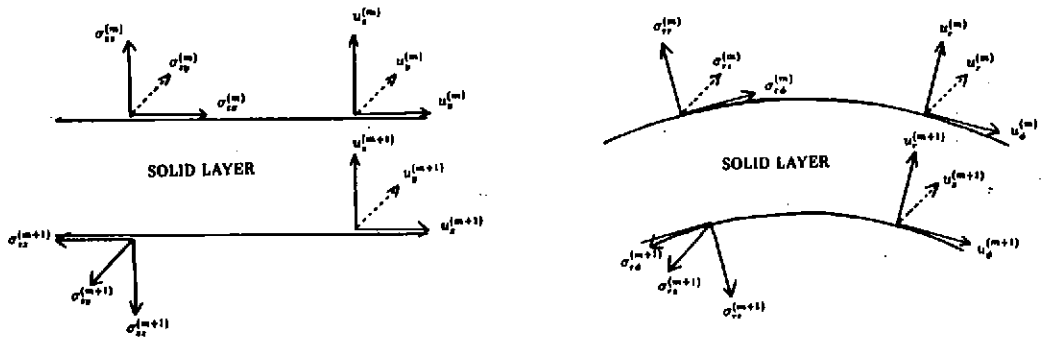

Figure 3: Stresses and Displacement Sign Conventions for Individual Layers

$$\begin{aligned}\mathbf{u}^{(m)} &= (\overline{u}_x^{(m)}(\alpha,\beta), \overline{u}_y^{(m)}(\alpha,\beta), \overline{u}_z^{(m)}(\alpha,\beta), \overline{u}_x^{(m+1)}(\alpha,\beta), \overline{u}_y^{(m+1)}(\alpha,\beta), \overline{u}_z^{(m+1)}(\alpha,\beta))^T, \\ \tilde{\boldsymbol{\sigma}}^{(m)} &= (\overline{\sigma}_{zx}^{(m)}(\alpha,\beta), \overline{\sigma}_{zy}^{(m)}(\alpha,\beta), \overline{\sigma}_{zz}^{(m)}(\alpha,\beta), \overline{\sigma}_{zx}^{(m+1)}(\alpha,\beta), \overline{\sigma}_{zy}^{(m+1)}(\alpha,\beta), \overline{\sigma}_{zz}^{(m+1)}(\alpha,\beta))^T,\end{aligned} \tag{1.6}$$

and for cylinders

$$\begin{aligned}\mathbf{u}^{(m)} &= (\overline{u}_z^{(m)}(n,\alpha), \overline{u}_\phi^{(m)}(n,\alpha), \overline{u}_r^{(m)}(n,\alpha), \overline{u}_z^{(m+1)}(n,\alpha), \overline{u}_\phi^{(m+1)}(n,\alpha), \overline{u}_r^{(m+1)}(n,\alpha))^T, \\ \tilde{\boldsymbol{\sigma}}^{(m)} &= (\overline{\sigma}_{rz}^{(m)}(n,\alpha), \overline{\sigma}_{r\phi}^{(m)}(n,\alpha), \overline{\sigma}_{rr}^{(m)}(n,\alpha), \overline{\sigma}_{rz}^{(m+1)}(n,\alpha), \overline{\sigma}_{r\phi}^{(m+1)}(n,\alpha), \overline{\sigma}_{rr}^{(m+1)}(n,\alpha))^T.\end{aligned} \tag{1.7}$$

For a system consisting of N layers these matrices can be assembled into a $(3N+3)\times(3N+3)$ system matrix, by eliminating the surface stresses, as

$$\mathbf{S}\mathbf{u} = \mathbf{E} \tag{1.8}$$

in which $\mathbf{u} = ((\overline{\mathbf{u}}^{(1)})^T, (\overline{\mathbf{u}}^{(2)})^T, \ldots, (\overline{\mathbf{u}}^{(N+1)})^T)^T$, $\mathbf{E}$ is the externally applied stress vector and the banded matrix $\mathbf{S}$ is

$$\begin{pmatrix}
-\mathbf{S}^e+\mathbf{S}_1^1 & \mathbf{S}_2^1 & & & & & & & & & \\
-\mathbf{S}_3^1 & -\mathbf{S}_4^1+\mathbf{S}_1^2 & \mathbf{S}_2^2 & & & & & & & & \\
 & -\mathbf{S}_3^2 & -\mathbf{S}_4^2+\mathbf{S}_1^3 & \mathbf{S}_2^3 & & & & & & & \\
 & & -\mathbf{S}_3^3 & -\mathbf{S}_4^3+\mathbf{S}_1^4 & \mathbf{S}_2^4 & & & & & & \\
 & & & \ddots & & & & & & & \\
 & & & & \ddots & & & & & & \\
 & & & & -\mathbf{S}_3^{N-3} & -\mathbf{S}_4^{N-3}+\mathbf{S}_1^{N-2} & \mathbf{S}_2^{N-2} & & & & \\
 & & & & & -\mathbf{S}_3^{N-2} & -\mathbf{S}_4^{N-2}+\mathbf{S}_1^{N-1} & \mathbf{S}_2^{N-1} & & & \\
 & & & & & & -\mathbf{S}_3^{N-1} & -\mathbf{S}_4^{N-1}+\mathbf{S}_1^{N} & \mathbf{S}_2^{N} & & \\
 & & & & & & & -\mathbf{S}_3^{N} & -\mathbf{S}_4^{N}+\mathbf{S}_1^{e} &
\end{pmatrix}$$

in which the individual matrices $\mathbf{S}^{(m)}$ have been partitioned into the 4 (3×3) submatrices $\mathbf{S}_1^m$, $\mathbf{S}_2^m$, $\mathbf{S}_3^m$ and $\mathbf{S}_4^m$, and $\mathbf{S}^e$ is a 3×3 matrix representing either the upper half-space or the exterior fluid, and $\mathbf{S}^i$ is a 3×3 matrix representing either the lower half-space or the interior fluid, details of which may be found elsewhere.

The vector $\mathbf{E}$ is the matrix of the applied spectral excitations. For a mechanical point force excitation applied to a layer boundary at (x_0, y_0, z_0) or, in cylindrical polar coordinates, (r_0, ϕ_0, z_0),

$$\mathbf{F} = \mathbf{F}_0\delta(x-x_0)\delta(y-y_0) = \mathbf{F}_0\delta(z-z_0)\delta(\phi-\phi_0)/r_0 \tag{1.9}$$

the spectral representations of which are easily obtained from the transform definitions as

$$\overline{\mathbf{F}}(\alpha,\beta) = \mathbf{F}_0\exp(-\mathrm{i}\alpha x_0 - \mathrm{i}\beta y_0) \tag{1.10}$$

for planar layers, or

$$\overline{\mathbf{F}}(n,\alpha) = \mathbf{F}_0\exp(-\mathrm{i}n\phi_0 - \mathrm{i}\alpha z_0)/2\pi r_0 \tag{1.11}$$

for cylindrical layers. The non-zero components of $\mathbf{E}$ are then the components of these spectral forces at the relevant layer boundary.

For an acoustic, rather than a mechanical excitation, it is convenient to express the pressure in the element containing the excitation, as

$$\overline{p} = \overline{p}_s + \overline{p}_r + \overline{p}_e \tag{1.12}$$

where $\overline{p}_s$ is the spectral form of the source term, $\overline{p}_r$ is the spectral form of the pressure scattered as though the element boundaries were rigid, and $\overline{p}_e$ is the spectral form of the pressure due to the normal motion of the layer boundaries. Hence, the spectral excitation on a boundary is $\overline{p}_s + \overline{p}_r$, with an appropriate sign to ensure that forces are positive when acting in the positive coordinate direction. Explicit expressions, omitted here,

for the point source and plane wave excitations may be found in [1] for planar layers and [2] for cylindrical layers.

Of interest in the acoustic problems considered here is the pressure in the upper half-space (or exterior fluid). For planar layers this pressure is related to the normal displacement of the upper boundary by

$$p_e(x,y,z) = \frac{\rho\omega^2}{4\pi^2 \mathrm{i}} \int_{-\infty}^{\infty}\int_{-\infty}^{\infty} \frac{U_t(\alpha,\beta)}{\gamma} \exp(\mathrm{i}\alpha x + \mathrm{i}\beta y + \mathrm{i}\gamma z)\mathrm{d}\alpha\mathrm{d}\beta \tag{1.13}$$

where $\gamma = \sqrt{k^2-\alpha^2-\beta^2}$, which may be evaluated immediately for plane wave incidence and otherwise whose far-field is found from the usual stationary phase approximation [5] as

$$p_f(R,\theta,\phi) = -\rho\omega^2 u_3(\overline{\alpha},\overline{\beta})\exp(\mathrm{i}kR)/2\pi R \tag{1.14}$$

where $\overline{\alpha} = k\sin\theta\cos\phi$ and $\overline{\beta} = k\sin\theta\sin\phi$. For cylindrical layers the external pressure is related to the normal displacement of the exterior boundary, $r = a$, by

$$p_e(r,\phi,z) = \frac{\rho\omega^2}{2\pi} \sum_{n=-\infty}^{\infty} \exp(\mathrm{i}n\phi) \int_{-\infty}^{\infty} \frac{U_t(n,\alpha)\mathrm{H}_{|n|}(\gamma r)\exp(\mathrm{i}\alpha z)\mathrm{d}\alpha}{\gamma \mathrm{H}'_{|n|}(\gamma a)} \tag{1.15}$$

in which $\gamma = \sqrt{k^2-\alpha^2}$, and whose far-field for non plane wave excitation is found [5] to be

$$p_f(R,\theta,\phi) = \frac{-\mathrm{i}\rho\omega^2\exp(\mathrm{i}kR)}{\pi kR\sin\theta} \sum_{n=-\infty}^{\infty} \frac{(-\mathrm{i})^{|n|}u_3(n,k\cos\theta)\exp(\mathrm{i}n\phi)}{\mathrm{H}'_{|n|}(ka\sin\theta)} \tag{1.16}$$

2 ANISOTROPIC PLANAR LAYERS

The scattering and/or radiation of sound from planar layered media, some layers of which may be anisotropic may be accomplished by using the analysis described in the previous section, provided that the matrix relating surface 'spectral' displacements and 'spectral' stresses for each individual layer can be obtained. Here it is assumed that the layer under consideration occupies the $x-y$ plane, $0 \le z \le h$, of a Cartesian coordinate system. Hence, the standard equations describing elastic motion may be expressed in terms of the stresses (σ) within the layer as

$$\partial\sigma_{xx}/\partial x + \partial\sigma_{xy}/\partial y + \partial\sigma_{xz}/\partial z = \rho\partial^2 u_x/\partial t^2, \quad \partial\sigma_{yx}/\partial x + \partial\sigma_{yy}/\partial y + \partial\sigma_{yz}/\partial z = \rho\partial^2 u_y/\partial t^2,$$
$$\partial\sigma_{zx}/\partial x + \partial\sigma_{zy}/\partial y + \partial\sigma_{zz}/\partial z = \rho\partial^2 u_z/\partial t^2, \tag{2.1}$$

where ρ is the density of the layer material. For linear elastic motions the stresses are related to the strains by the matrix equation

$$\begin{pmatrix} \sigma_{xx} \\ \sigma_{yy} \\ \sigma_{zz} \\ \sigma_{xy} \\ \sigma_{yz} \\ \sigma_{zx} \end{pmatrix} = \begin{pmatrix} d_{11} & d_{12} & d_{13} & d_{14} & d_{15} & d_{16} \\ d_{12} & d_{22} & d_{23} & d_{24} & d_{25} & d_{26} \\ d_{13} & d_{23} & d_{33} & d_{34} & d_{35} & d_{36} \\ d_{14} & d_{24} & d_{34} & d_{44} & d_{45} & d_{46} \\ d_{15} & d_{25} & d_{35} & d_{45} & d_{55} & d_{56} \\ d_{16} & d_{26} & d_{36} & d_{46} & d_{56} & d_{66} \end{pmatrix} \begin{pmatrix} \varepsilon_{xx} \\ \varepsilon_{yy} \\ \varepsilon_{zz} \\ \varepsilon_{xy} \\ \varepsilon_{yz} \\ \varepsilon_{zx} \end{pmatrix} \tag{2.2}$$

in which the symmetric 6×6 matrix above contains 21 elastic constants. The number of independent constants is governed by the microscopic structure of the material. For example orthotropic material has 9 independent constants and isotropic material only 2. The standard definitions for the strains (ε),

$$\varepsilon_{xx} = \partial u_x/\partial x, \qquad \varepsilon_{yy} = \partial u_y/\partial y, \qquad \varepsilon_{zz} = \partial u_z/\partial z,$$
$$\varepsilon_{xy} = \partial u_x/\partial y + \partial u_y/\partial x, \quad \varepsilon_{yz} = \partial u_y/\partial z + \partial u_z/\partial y, \quad \varepsilon_{zx} = \partial u_z/\partial x + \partial u_x/\partial z \tag{2.3}$$

THEORETICAL METHODS FOR FIBRE-REINFORCED MATERIALS

have been used above. Using the inverse Fourier transform expression (1.2) for the displacement allows the operators $\partial/\partial x$ and $\partial/\partial y$ to be replaced by the factors $i\alpha$ and $i\beta$, respectively. Substitution of this expression for the displacement, firstly into equation (2.3) to obtain the strains, then into (2.2) to obtain the stresses and finally into (2.1) results in the transformed equation of motion for the layer:

$$\left(-\mathbf{X}\frac{\partial^2}{\partial z^2} - i\mathbf{Y}(\alpha,\beta)\frac{\partial}{\partial z} + \mathbf{Z}(\alpha,\beta)\right)\begin{pmatrix}\overline{u}_x(\alpha,\beta,z)\\ \overline{u}_y(\alpha,\beta,z)\\ \overline{u}_z(\alpha,\beta,z)\end{pmatrix} = \begin{pmatrix}0\\0\\0\end{pmatrix} \tag{2.4}$$

where $\mathbf{X}$, $\mathbf{Y}(\alpha,\beta)$ and $\mathbf{Z}(\alpha,\beta)$ are 3×3 matrices. This is the matrix form of a second order differential equation with respect to z, with constant (with respect to z) coefficients. Hence its solutions are known to be of the form

$$\begin{pmatrix}\tilde{u}_x(\alpha,\beta,\gamma)\\ \tilde{u}_y(\alpha,\beta,\gamma)\\ \tilde{u}_z(\alpha,\beta,\gamma)\end{pmatrix} e^{i\gamma z} \tag{2.5}$$

for certain values of γ. These are found by first substituting the trial solution (2.5) into the propagation matrix equation (2.4) to obtain

$$\left(\gamma^2\mathbf{X} + \gamma\mathbf{Y}(\alpha,\beta) + \mathbf{Z}(\alpha,\beta)\right)\begin{pmatrix}\tilde{u}_x(\alpha,\beta,\gamma)\\ \tilde{u}_y(\alpha,\beta,\gamma)\\ \tilde{u}_z(\alpha,\beta,\gamma)\end{pmatrix} = \mathbf{D}(\alpha,\beta,\gamma)\begin{pmatrix}\tilde{u}_x(\alpha,\beta,\gamma)\\ \tilde{u}_y(\alpha,\beta,\gamma)\\ \tilde{u}_z(\alpha,\beta,\gamma)\end{pmatrix} = \begin{pmatrix}0\\0\\0\end{pmatrix} \tag{2.6}$$

which has non-trivial solutions $\tilde{\mathbf{u}}$ only when the determinant of the matrix $\mathbf{D}$ vanishes, i.e.,

$$|\mathbf{D}(\alpha,\beta,\gamma)| = 0. \tag{2.7}$$

This is a sixth order polynomial for γ. For the general case when the material has 21 elastic constants these roots must be found numerically, but in the special cases of orthotropic or isotropic materials it may be written as a cubic equation for γ^2, whose roots can be found analytically. For each of these roots γ_j a corresponding solution vector $\tilde{\mathbf{u}}(\alpha,\beta,\gamma_j)$ can also be found from equation (2.6). Hence the general solution for the displacement within the layer is a linear combination of all these solutions,

$$\begin{pmatrix}\overline{u}_x(\alpha,\beta,z)\\ \overline{u}_y(\alpha,\beta,z)\\ \overline{u}_z(\alpha,\beta,z)\end{pmatrix} = \sum_{j=1}^{6} A_j \begin{pmatrix}\tilde{u}_x(\alpha,\beta,\gamma_j)\\ \tilde{u}_y(\alpha,\beta,\gamma_j)\\ \tilde{u}_z(\alpha,\beta,\gamma_j)\end{pmatrix} e^{i\gamma_j z} \tag{2.8}$$

from which the 'spectral' displacements at the layer boundaries $z = h$ and $z = 0$ may be written in matrix notation as

$$\mathbf{u}^{(m)}(\alpha,\beta) = \mathbf{R}(\alpha,\beta)\mathbf{A} \tag{2.9}$$

Further substitution of the solution (2.8) into equations (2.2) and (2.3) also allows the 'spectral' stresses within the layer to be written in terms of the coefficients A_j, and in particular specializing these to the layer boundaries results in another matrix equation

$$\tilde{\boldsymbol{\sigma}}^{(m)}(\alpha,\beta) = \mathbf{P}(\alpha,\beta)\mathbf{A} \tag{2.10}$$

Finally, eliminating $\mathbf{A}$ from equations (2.9) and (2.10) results in the required matrix equation for the layer

$$\mathbf{P}(\alpha,\beta)\mathbf{R}^{-1}(\alpha,\beta)\mathbf{u}^{(m)}(\alpha,\beta) = \mathbf{S}^{(m)}(\alpha,\beta)\mathbf{u}^{(m)}(\alpha,\beta) = \tilde{\boldsymbol{\sigma}}^{(m)}(\alpha,\beta). \tag{2.11}$$

Some effects of anisotropy upon the acoustic properties are illustrated in Figure 4. This shows the plane wave reflection coefficient, as a function of both frequency and angle of incidence, θ. In each of these plots the

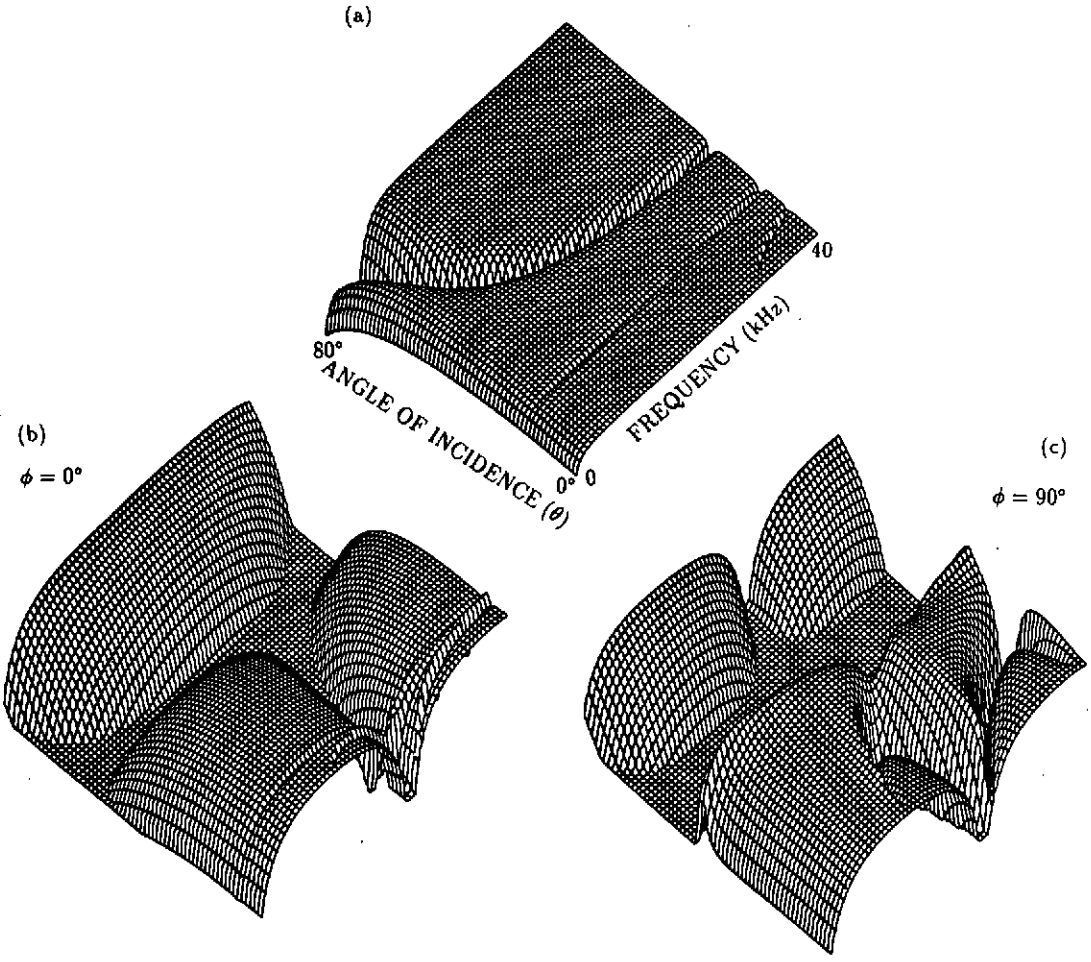

Figure 4: Plane Wave Reflection Coefficient
(a) Isotropic Steel Plate, (b) CFRP Plate $\phi = 0°$, (c) CFRP Plate $\phi = 90°$.

frequency range is 0 - 40kHz and the incidence angle varies from 0° (normal incidence) to 80°. The maximum level for each plot is 0dB, and the surface plots are clipped at -20dB, leading to an artificial flat base. Figure 4a is obtained for a 5cm thick isotropic steel plate in water. In Figures 4b and 4c the plate is a carbon fibre reinforced plastic (CFRP), with stiffening fibres oriented along the $x-$axis, such that the Young's modulus for the material in the $x-$direction is approximately that of steel, but has only 1/27 of that value in the y and z directions. The reflection coefficient is independent of the azimuthal angle, ϕ, for the isotropic steel plate. Figure 4b shows the reflection coefficient for $\phi = 0°$ (i.e. incidence in the plane of the stiffening fibres) for the CFRP plate, and 4c shows $\phi = 90°$ (i.e. incidence in the plane perpendicular to the stiffening fibres). The anisotropy results in significant differences both between these two plots, and the plot for the isotropic steel plate. In particular, for this example, the flat base is evident for the CFRP plate for a range of frequencies and angles, indicating a very low reflection coefficient (< -20dB) there. A detailed physical explanation of the features of the plots is outside the scope of this paper.

3 ANISOTROPIC CYLINDRICAL LAYERS

Another geometry, frequently of interest, is that of concentric cylindrical layers. If some of these layers are anisotropic, with the anisotropy cylindrical in character, then equation (2.2) relating stresses and strains in an anisotropic planar layer is replaced by

$$\begin{pmatrix} \sigma_{zz} \\ \sigma_{\phi\phi} \\ \sigma_{rr} \\ \sigma_{z\phi} \\ \sigma_{\phi r} \\ \sigma_{rz} \end{pmatrix} = \begin{pmatrix} d_{11} & d_{12} & d_{13} & d_{14} & d_{15} & d_{16} \\ d_{12} & d_{22} & d_{23} & d_{24} & d_{25} & d_{26} \\ d_{13} & d_{23} & d_{33} & d_{34} & d_{35} & d_{36} \\ d_{14} & d_{24} & d_{34} & d_{44} & d_{45} & d_{46} \\ d_{15} & d_{25} & d_{35} & d_{45} & d_{55} & d_{56} \\ d_{16} & d_{26} & d_{36} & d_{46} & d_{56} & d_{66} \end{pmatrix} \begin{pmatrix} \varepsilon_{zz} \\ \varepsilon_{\phi\phi} \\ \varepsilon_{rr} \\ \varepsilon_{z\phi} \\ \varepsilon_{\phi r} \\ \varepsilon_{rz} \end{pmatrix} \tag{3.1}$$

in cylindrical polar coordinates. For the cylindrical geometry the method used in the planar case for solving the equations of motion results in a second order, 3×3 matrix, differential equation whose coefficients are functions of r, and whose general solution is not immediately obvious. An exact solution in terms of Bessel functions has been obtained for a special case of axial stiffening only.

A numerical procedure has however been utilized to obtain results with such cylindrically anisotropic layers. This involves assuming first that the 'spectral' displacement across the layer thickness can be approximated by a quadratic function of the radial coordinate,

$$\begin{pmatrix} \overline{u}_z(r,n,\alpha) \\ \overline{u}_\phi(r,n,\alpha) \\ \overline{u}_r(r,n,\alpha) \end{pmatrix} = \begin{pmatrix} 1 & r & r^2 & 0 & 0 & 0 & 0 & 0 & 0 \\ 0 & 0 & 0 & 1 & r & r^2 & 0 & 0 & 0 \\ 0 & 0 & 0 & 0 & 0 & 0 & 1 & r & r^2 \end{pmatrix} \begin{pmatrix} \beta_1 \\ \beta_2 \\ \beta_3 \\ \beta_4 \\ \beta_5 \\ \beta_6 \\ \beta_7 \\ \beta_8 \\ \beta_9 \end{pmatrix} \tag{3.2}$$

and minimizing the energy functional

$$\begin{aligned} \Pi \;=\; & \frac{1}{2}\int_{-\infty}^{\infty}\int_{0}^{2\pi}\int_{a}^{b} [\boldsymbol{\varepsilon}^*(r,\phi,z)^T\boldsymbol{\sigma}(r,\phi,z) + \rho\dot{\mathbf{u}}^*(r,\phi,z)^T\dot{\mathbf{u}}(r,\phi,z)]r\mathrm{d}r\mathrm{d}\phi\mathrm{d}z \\ & -b\int_{-\infty}^{\infty}\int_{0}^{2\pi}\mathbf{u}^*(b,\phi,z)^T\mathbf{F}(b,\phi,z)\mathrm{d}\phi\mathrm{d}z - a\int_{-\infty}^{\infty}\int_{0}^{2\pi}\mathbf{u}^*(a,\phi,z)^T\mathbf{F}(a,\phi,z)\mathrm{d}\phi\mathrm{d}z \end{aligned} \tag{3.3}$$

for the layer. The first term is potential energy, the second term is kinetic energy and the final terms are work done by the surface stresses $\overline{\mathbf{F}}$. By using the Fourier integral and series transformations (1.4) for the displacement, the axial and circumferential integrations in the definition of Π are straightforward, leaving Π as an integral across the layer thickness of the 'spectral' quantities with respect to r.

As the standard definitions for strains in cylindrical polar coordinates are

$$\begin{aligned} \varepsilon_{zz} &= \partial u_z/\partial z, \qquad \varepsilon_{\phi\phi} = \partial u_\phi/r\partial\phi + u_r/r, \qquad \varepsilon_{rr} = \partial u_r/\partial r, \\ \varepsilon_{z\phi} &= \partial u_\phi/\partial z + \partial u_z/r\partial\phi, \quad \varepsilon_{\phi r} = \partial u_r/r\partial\phi + \partial u_\phi/\partial r - u_\phi/r, \quad \varepsilon_{rz} = \partial u_r/\partial z + \partial u_z/\partial r \end{aligned} \tag{3.4}$$

it is clear that each component of both $\boldsymbol{\varepsilon}$ and $\boldsymbol{\sigma}$ is a linear combination of the coefficients β_i. Thus Π contains terms of the form $\beta_i\beta_j$ and β_i. Hence minimizing Π with respect to each β_i in turn leads to a set of nine linear

equations for the β_i, $i = 1,9$. The β_i can be related to the spectral displacements at the layer boundaries, by evaluating equation (3.2) at $r = b$, $r = a$ and at some other position within the layer, $r = c = (a+b)/2$ for example,

$$\hat{\mathbf{u}}(n,\alpha) = \begin{pmatrix} \overline{u}_z(b,n,\alpha) \\ \overline{u}_\phi(b,n,\alpha) \\ \overline{u}_r(b,n,\alpha) \\ \overline{u}_z(c,n,\alpha) \\ \overline{u}_\phi(c,n,\alpha) \\ \overline{u}_r(c,n,\alpha) \\ \overline{u}_z(a,n,\alpha) \\ \overline{u}_\phi(a,n,\alpha) \\ \overline{u}_r(a,n,\alpha) \end{pmatrix} = \begin{pmatrix} 1 & b & b^2 & 0 & 0 & 0 & 0 & 0 & 0 \\ 0 & 0 & 0 & 1 & b & b^2 & 0 & 0 & 0 \\ 0 & 0 & 0 & 0 & 0 & 0 & 1 & b & b^2 \\ 1 & c & c^2 & 0 & 0 & 0 & 0 & 0 & 0 \\ 0 & 0 & 0 & 1 & c & c^2 & 0 & 0 & 0 \\ 0 & 0 & 0 & 0 & 0 & 0 & 1 & c & c^2 \\ 1 & a & a^2 & 0 & 0 & 0 & 0 & 0 & 0 \\ 0 & 0 & 0 & 1 & a & a^2 & 0 & 0 & 0 \\ 0 & 0 & 0 & 0 & 0 & 0 & 1 & a & a^2 \end{pmatrix} \begin{pmatrix} \beta_1 \\ \beta_2 \\ \beta_3 \\ \beta_4 \\ \beta_5 \\ \beta_6 \\ \beta_7 \\ \beta_8 \\ \beta_9 \end{pmatrix} \tag{3.5}$$

Hence the result of minimizing Π can be expressed as a linear equation for these spectral displacements:

$$\hat{\mathbf{S}}(n,\alpha)\hat{\mathbf{u}}(n,\alpha) = \hat{\mathbf{F}}(n,\alpha), \tag{3.6}$$

in which the elements of $\hat{\mathbf{S}}$ are integrals across the layer thickness of polynomial functions of r whose coefficients are known, and which can be evaluated either numerically, or analytically to minimize computer time, and $\hat{\mathbf{F}}(n,\alpha) = (b\overline{F}_z(b,n,\alpha), b\overline{F}_\phi(b,n,\alpha), b\overline{F}_r(b,n,\alpha), 0, 0, 0, a\overline{F}_z(a,n,\alpha), a\overline{F}_\phi(a,n,\alpha), a\overline{F}_r(a,n,\alpha))^T$. The required 6×6 matrix $\mathbf{S}(n,\alpha)$ may be obtained by inverting equation (3.6), thus expressing the spectral displacements in terms of the surface spectral stresses as

$$\hat{\mathbf{u}}(n,\alpha) = \hat{\mathbf{S}}^{-1}(n,\alpha)\hat{\mathbf{F}}(n,\alpha). \tag{3.7}$$

By deleting the unwanted components of displacement (those at $r = c$), this can be expressed in terms of the surface spectral stresses as

$$\mathbf{u}^{(m)}(n,\alpha) = \mathbf{S}^{(m)^{-1}}(n,\alpha)\hat{\boldsymbol{\sigma}}^{(m)}(n,\alpha) \tag{3.8}$$

which when inverted gives the required matrix equation (1.5) for the layer.

Except at very low frequencies or for very thin layers the quadratic variation of the displacement across the layer thickness assumed above is unlikely to prove accurate, so the layer should first be subdivided into a suitably large number of sublayers which are sufficiently thin, and the procedure outlined above followed for each sublayer, before finally discarding the displacements at all but the boundaries of the original layer. The computer program should be designed to do this automatically.

The numerical results of Figure 5 were obtained from this procedure. This compares the backscattered pressure at normal incidence for a 5cm thick cylindrical steel shell, outer radius 5m, immersed in water but containing no interior fluid (shown by the dotted line), with that for a CFRP shell with axial stiffening (5a) or circumferential stiffening (5b). At low frequencies the circumferential stiffness controls the scattering, hence in Figure 5a the scattering from the axially stiffened CFRP shell is much greater than that from the steel shell due to the much lower value of Young's modulus in the circumferential direction. In Figure 5b the low frequency scattering from the circumferentially stiffened CFRP shell is almost identical to that from the steel shell due to the approximately equal values for Young's modulus in the circumferential direction. Detailed physical explanations of the other features of these plots is outside the scope of this paper.

4 RIB STIFFENED SHELL

The procedures outlined above allow prediction of the acoustic characteristics of layered shells subjected to various excitations. In this section the layered cylindrical system is stiffened by an infinite number of equally

THEORETICAL METHODS FOR FIBRE-REINFORCED MATERIALS

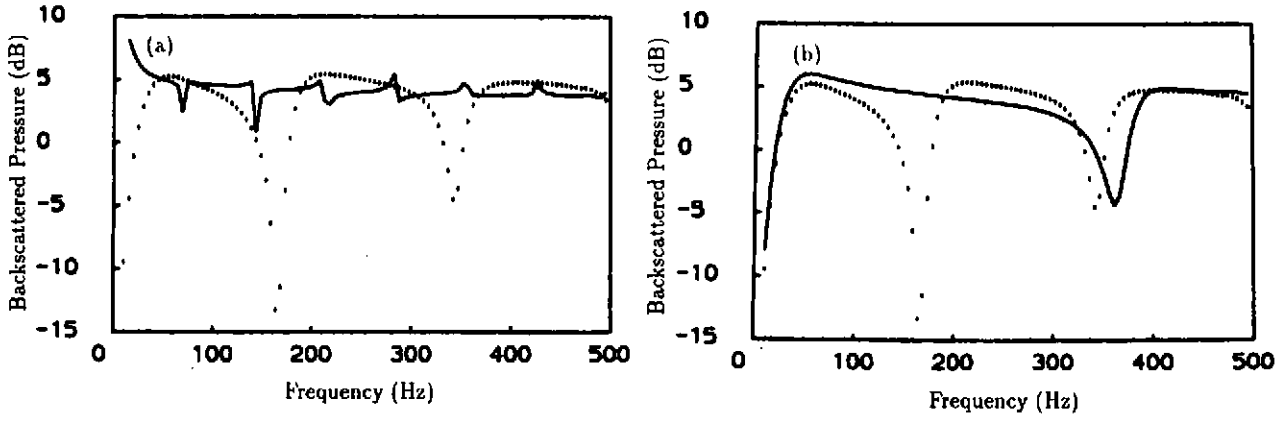

Figure 5: Backscattered Pressure at Normal Incidence
(a) Isotropic Steel Shell $\cdots$, CFRP shell with axial stiffening ——
(b) Isotropic Steel Shell $\cdots$, CFRP shell with circumferential stiffening ——.

spaced identical axisymmetric ribs, which each exert unknown reaction forces and a bending moment on the layered system. Hence for each rib, the relation between the reaction forces applied to the cylinder (opposite to those applied to the rib), and the displacement of the rib at the cylinder (the same as that of the cylinder there) may be expressed in terms of the spectral stiffness matrix $\mathbf{B}$ for the ribs as

$$\mathbf{B}(n)\mathbf{u}(n, qd) = -\mathbf{F}(n, qd) \tag{4.1}$$

where the ribs are located, with spacing d at $z = qd$, $q = 0, \pm 1, \pm 2, \ldots$. The unstiffened cylinder has the usual spectral matrix equation

$$\mathbf{S}(n, \alpha)\mathbf{u}(n, \alpha) = \mathbf{E}_S(n, \alpha) \tag{4.2}$$

in which the excitation $\mathbf{E}_S$ includes the excitations of the reaction forces and moments due to the ribs, and which may be rewritten in slightly augmented form, so that explicit expressions are available for the transform of $\partial u_r/\partial z$ in terms not only of the reaction forces, but also explicitly in terms of the reaction moment,

$$\underset{(4 \times 4)}{\mathbf{u}_D(n, \alpha) = \mathbf{D}(n, \alpha)} \ \mathbf{E}_D(n, \alpha). \tag{4.3}$$

The solution for the spectral displacement of the periodically stiffened cylinder may be obtained explicitly, after some algebra, by making use of the Poisson summation theorem and eliminating the reaction forces and moments due to the ribs, as

$$\mathbf{u}_D(n, \alpha) = \mathbf{D}(n, \alpha)\mathbf{E}_D(n, \alpha) - (1/d)\mathbf{D}(n, \alpha)\mathbf{B}(n)\times$$

$$\left[\mathbf{I} + \left(\frac{1}{d}\right) \sum_{q=-\infty}^{\infty} \mathbf{D}(n, \alpha + \frac{2\pi q}{d})\mathbf{B}(n)\right]^{-1} \sum_{q=-\infty}^{\infty} \mathbf{D}(n, \alpha + \frac{2\pi q}{d})\mathbf{E}_D(n, \alpha + \frac{2\pi q}{d}). \tag{4.4}$$

It is clear from this expression that for each evaluation of the scattered or radiated pressure several, possibly many, evaluations of $\mathbf{S}$ are required. Using the theory of the previous section each of the calculations of $\mathbf{S}$ may themselves involve a fairly lengthy computation. In addition the pressure field is a complicated function of position, and in order to describe it fully evaluations at many locations may be required. A useful indicator

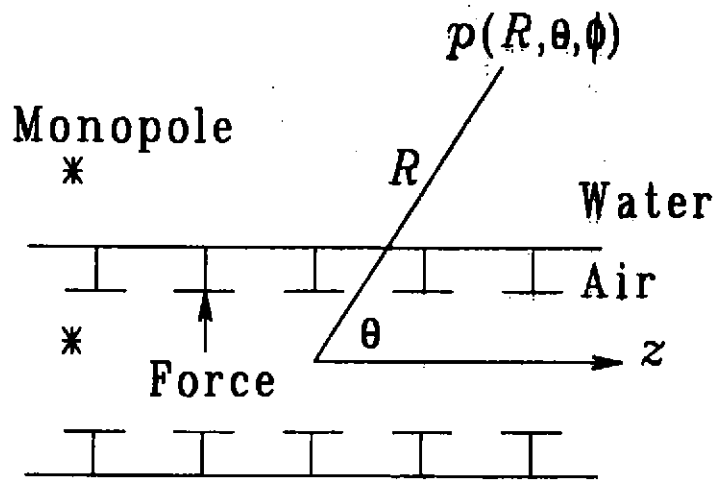

Figure 6: Rib Stiffened Shell Geometry

of the acoustic characteristics of the system is the total radiated or scattered sound power, which smooths out the spatial variation, but whose calculation requires an additional (numerical) integration.

To reduce computation times substantially the cylindrical system can be modelled, not by the 'exact' theory described in the previous section, but as an anisotropic shell. Instead of working with the displacements at each of the layer boundaries the shell is described only by its displacement at its mean radius a. When transverse shear and rotary inertia are neglected the laminated composite shallow shell equations of Leissa & Qatu [6] result in the (3×3) spectral dynamic stiffness equation in which

$$
\begin{aligned}
S_{11} &= \left[A_{66}n^2/a^2 + 2A_{26}\alpha n/a + A_{22}\alpha^2\right] - \rho_s h\omega^2, \\
S_{12} &= \left[A_{16}n^2/a^2 + (A_{12}+A_{66})\alpha n/a + A_{26}\alpha^2\right], \\
S_{13} &= -\mathrm{i}\left[B_{16}n^3/a^3 + 3B_{26}\alpha^2 n/a + (B_{12}+2B_{66})n^2\alpha/a^2 + B_{22}\alpha^3 + A_{12}\alpha/a + A_{16}n/a^2\right], \\
S_{22} &= \left[A_{11}n^2/a^2 + 2A_{16}n\alpha/a + A_{66}\alpha^2\right] - \rho_s h\omega^2, \\
S_{23} &= -\mathrm{i}\left[B_{11}n^3/a^3 + 3B_{16}n^2\alpha/a^2 + (B_{12}+2B_{66})\alpha^2 n/a + B_{26}\alpha^3 + A_{11}n/a^2 + A_{16}\alpha/a\right], \\
S_{33} &= \left[D_{11}n^4/a^4 + 4D_{16}n^3\alpha/a^3 + 2(D_{12}+D_{66})n^2\alpha^2/a^2 + 4D_{26}n\alpha^3/a + \right. \\
&\quad D_{22}\alpha^4 + 2B_{11}n^2/a^3 + 4B_{16}n\alpha/a^2 + 2B_{12}\alpha^2/a + A_{11}/a^2\left.\right] - \rho_s h\omega^2 + \\
&\quad \rho_e\omega^2 \mathrm{H}_n(\gamma_e a)/\gamma_e \mathrm{H}_n'(\gamma_e a) - \rho_i\omega^2 \mathrm{J}_n(\gamma_i a)/\gamma_i \mathrm{J}_n'(\gamma_i a)
\end{aligned}
\tag{4.5}
$$

which reduce, for a single isotropic layer, to the usual Donnell-Mushtari shell equations [5]. The stiffness values A_{ij}, B_{ij} and D_{ij} are found by first identifying $\overline{x}$ and $\overline{y}$ axes with the local circumferential and z axes for each layer so that for unidirectional fibre-reinforcement within this plane the in-plane stress-strain relations can be written

$$
\begin{pmatrix} \overline{\sigma}_{\overline{x}\overline{x}} \\ \overline{\sigma}_{\overline{y}\overline{y}} \\ \overline{\sigma}_{\overline{x}\overline{y}} \end{pmatrix} = \begin{pmatrix} \overline{Q}_{11} & \overline{Q}_{12} & \overline{Q}_{16} \\ \overline{Q}_{12} & \overline{Q}_{22} & \overline{Q}_{26} \\ \overline{Q}_{16} & \overline{Q}_{26} & \overline{Q}_{66} \end{pmatrix} \begin{pmatrix} \overline{\varepsilon}_{\overline{x}\overline{x}} \\ \overline{\varepsilon}_{\overline{y}\overline{y}} \\ \overline{\varepsilon}_{\overline{x}\overline{y}} \end{pmatrix} \tag{4.6}
$$

where the coefficients $\overline{Q}$ may be obtained from mixture theories together with a transformation to account for the stacking angle of the fibres within the layer. The constants for the shell are obtained by summing the

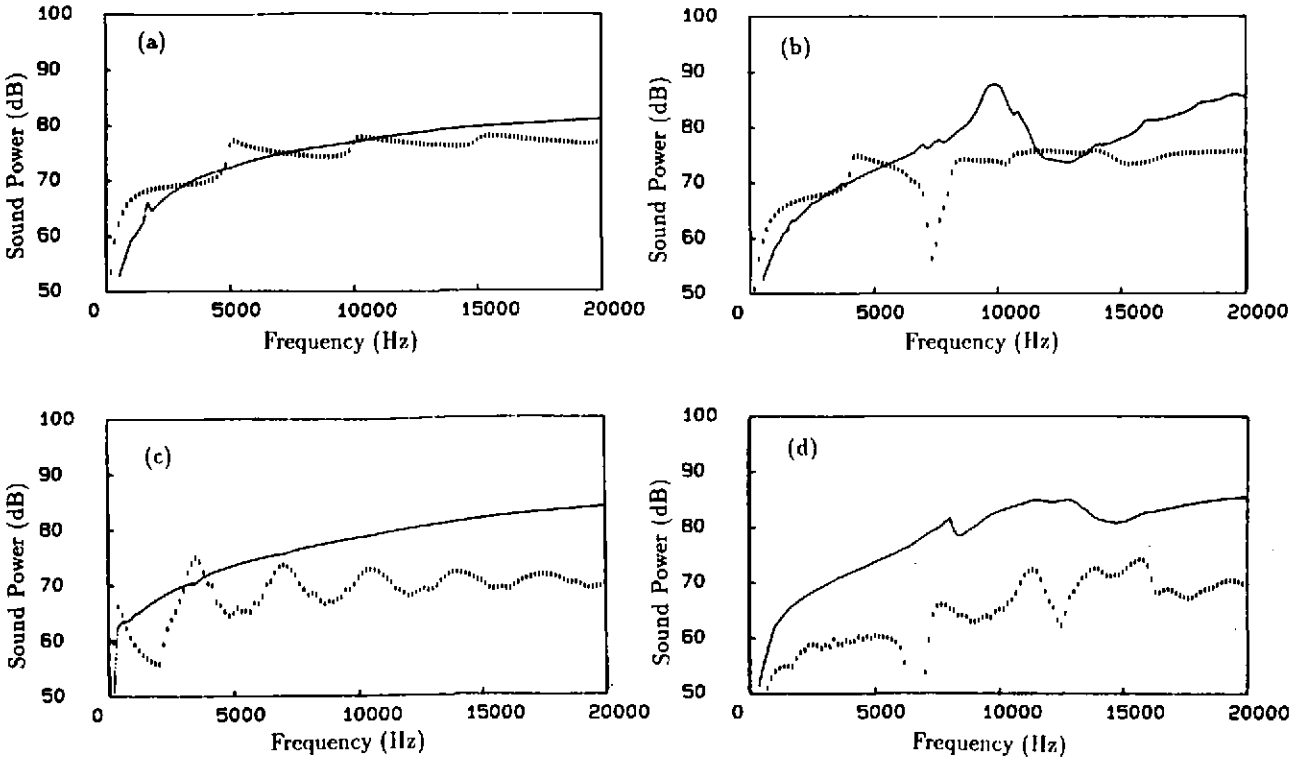

Figure 7: Acoustic Power in Water due to Radial (——) and Axial (· · ·) Point Force Excitation
(a) Steel Shell, No Ribs, (b) Steel Shell With Ribs
(c) Axially Reinforced CFRP Shell, No Ribs, (d) Axially Reinforced CFRP Shell With Ribs.

value of these quantities for each of the thin layers which compose the laminated anisotropic shell. Hence,

$$A_{ij} = \sum_{m=1}^{M} \overline{Q}_{ij}^{(m)}(t_m - t_{m-1}), \quad B_{ij} = \tfrac{1}{2}\sum_{m=1}^{M} \overline{Q}_{ij}^{(m)}(t_m^2 - t_{m-1}^2),$$
$$D_{ij} = \tfrac{1}{3}\sum_{m=1}^{M} \overline{Q}_{ij}^{(m)}(t_m^3 - t_{m-1}^3), \quad \rho_s = \tfrac{1}{h}\sum_{m=1}^{M} \rho^{(m)}(t_m - t_{m-1}), \tag{4.7}$$

where $t_m = z_m - z_c$ with z_m the $\overline{z}$ coordinate of the upper surface of the mth layer, and z_c the $\overline{z}$ coordinate of the laminates midsurface.

The ribs stiffening the laminated shell have been modelled by using a finite element procedure to assemble axisymmetric conical shell elements. The stiffnesses for each element are calculated in the same way as those of the laminated cylindrical shell, outlined above.

Figure 7 shows an example of the effects of equally spaced ribs, and compares the effect on the acoustic power radiated in water due to a radial or an axial force applied to a rib connection point, for a steel shell and a CFRP shell with axial reinforcement. In this example the shell radius is 10cm and the thickness 0.2cm. When the excitation is a radial force the power levels from the CFRP shell are slightly higher than those from the steel shell, but for the axial force the level of the steel shell is higher.

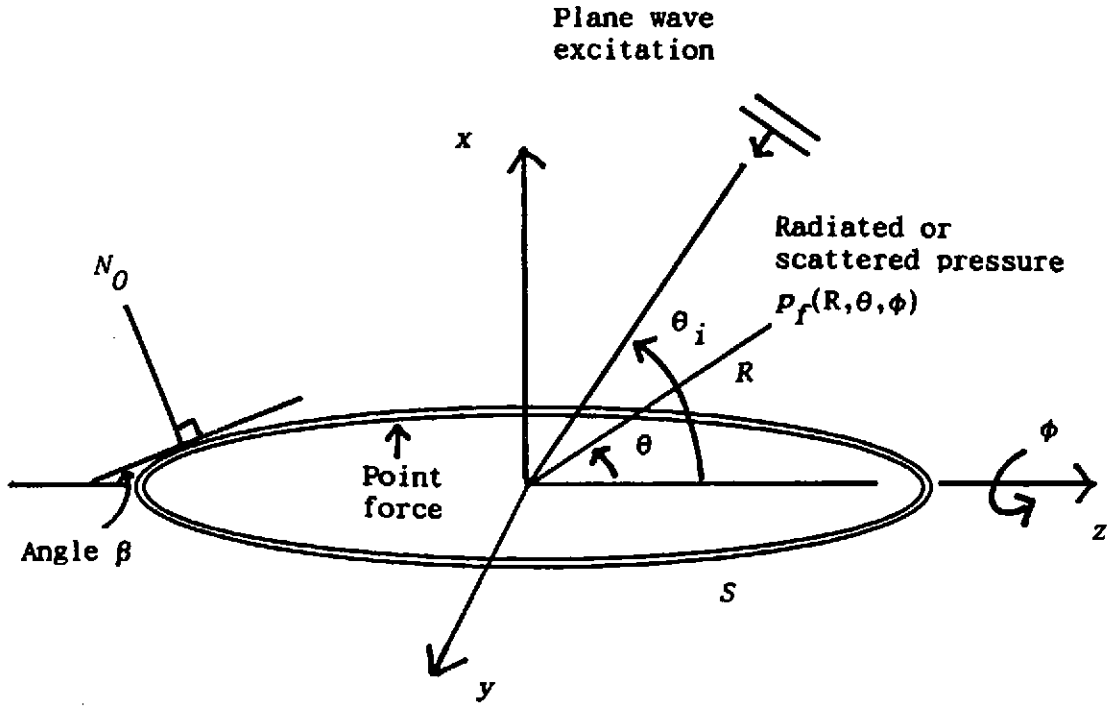

Figure 8: Geometry and Co-ordinate Systems For a Finite Axisymmetric Structure

5 FINITE AXISYMMETRIC STRUCTURES

A finite axisymmetric anisotropic structure has been modelled both by laminated composite shell finite elements, and by anisotropic axisymmetric solid elements. The theory for conical shell elements is useful when the variation through the shell thicknesses of the field quantities is small. For such an element a cubic variation with distance along the shell is assumed for the normal displacement and a linear variation for both the circumferential displacement and the displacement along the shell. A procedure similar to that outlined in the cylindrical layers section of this paper results, for each circumferential harmonic, in a matrix relating the displacements of the ends of the element to the forces applied there. Such element matrices can then be assembled, reflecting continuity of displacement, to form a matrix equation relating the displacements of each end of each element to the external forces applied to the element boundaries.

For the axisymmetric solid element, displacements are assumed to vary quadratically with both radius and axial distance, for each harmonic, and hence a 9-noded element is required to provide the 27 displacements corresponding to the 27 unknown coefficients. Use of the constitutive equation (3.1) and a minimization, similar to that of section 3, with respect to the unknown coefficients provides a suitable matrix equation relating displacements and forces at the element boundaries in the absence of fluid loading. Extracting the relation between normal forces and excitations from this it can be written in the usual form, for each harmonic, as

$$\mathbf{S}(n)\mathbf{W}(n) = \mathbf{E}(n) \tag{5.1}$$

where $\mathbf{S}$ is an $m \times m$ matrix if the structure is divided into $m-1$ axisymmetric elements. Fluid loading effects are accounted for by using the Helmholtz integral formula, which relates the radiated pressure in the exterior fluid to an integral over the body surface of both the pressure combined with the normal gradient of the Green's function and the normal displacement combined with the Green's function. Discretizing this

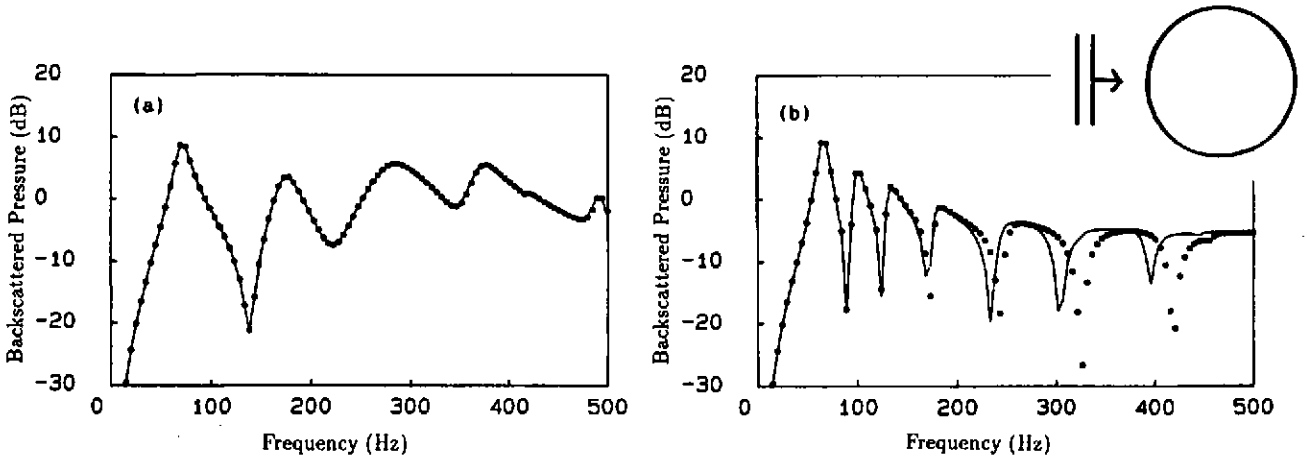

Figure 9: Backscattered Pressure from an Anisotropic Spherical Shell,
• Conical Shell Model, ____ Axisymmetric Solid Model
(a) Circumferential Reinforcement, (b) Meridional Reinforcement

allows the nodal pressures to be related to the normal displacements, hence

$$\mathbf{P}(n) = \mathbf{D}(n)\mathbf{W}(n). \tag{5.2}$$

The nodal forces are obtained by integrating the pressures over a suitable area,

$$\mathbf{F}(n) = -\mathbf{A}\mathbf{P}(n). \tag{5.3}$$

Thus with exterior fluid loading the shell finite element equation (5.1) becomes

$$[\mathbf{S}(n) + \mathbf{A}\mathbf{D}(n)]\mathbf{W}(n) = \mathbf{E}(n) - \mathbf{A}[\mathbf{P}_i(n) + \mathbf{P}_r(n)] \tag{5.4}$$

where $\mathbf{E}(n)$ is the vector of externally applied nodal forces, $\mathbf{P}_i(n)$ is the vector of nodal pressures due to any incident acoustic pressure and $\mathbf{P}_r(n)$ is the vector of nodal pressures due to the rigid reflection at the surface of such an incident wave,

$$\mathbf{P}_r(n) = -\mathbf{D}(n)\mathbf{W}_i(n) \tag{5.5}$$

where $\mathbf{W}_i$ is the nodal displacement in the fluid due to the incident wave alone. Equation (5.4) can be inverted to calculate $\mathbf{W}(n)$, the nodal displacement of the structure due to its elastic motion. A further application of the Helmholtz integral formula using the nodal surface displacement $\mathbf{W}(n) - \mathbf{W}_i(n)$, and the nodal surface pressure $\mathbf{D}(n)[\mathbf{W}(n) - \mathbf{W}_i(n)]$ gives the scattered or radiated sound pressure.

Numerical tests show close agreement between values obtained using this theory and exact theory for a rigid spherical shell, and for an isotropic spherical shell at low frequencies, but poorer agreement as the frequency increases, probably due to the need to increase the number of elements at the higher frequencies. Figure 9 shows some results obtained for the backscattered pressure for an empty CFRP spherical shell of radius 1m and thickness 1cm, in water. Figure 9a shows results obtained from both models for fibre reinforcement in the circumferential direction. There is good agreement. The results of meridional stiffening is shown in Figure 9b. The two models agree well at low frequencies but diverge as the frequency increases.

6 ACKNOWLEDGEMENT

This work has been carried out with the support of the Procurement Executive, Ministry of Defence.

7 REFERENCES

[1] E. A. SKELTON & J. H. JAMES 'Acoustics of anisotropic planar layered media', *Journal of Sound and Vibration* **152**, pp157-174 (1992).

[2] E. A. SKELTON & J. H. JAMES 'Acoustics of an anisotropic layered cylinder', *Journal of Sound and Vibration* **161**, pp251-264 (1993).

[3] J. H. JAMES 'Sound radiation from infinite laminated composite shell with periodic rib stiffening', *DRA Haslar Gosport Hants PO12 2AG* **DRA/TM(USGR)92326** (1992).

[4] J. H. JAMES 'Low frequency acoustics of laminated composite axisymmetric structures', *DRA Haslar Gosport Hants PO12 2AG* **DRA/TM(USGR)93302** (1993).

[5] M. C. JUNGER & D. FEIT 'Sound, Structures and Their Interaction' (second edition) Cambridge, Massachusetts: MIT Press (1986).

[6] A. W. LEISSA & M. S. QATU 'Equations of elastic deformation of laminated composite shallow shells', *Journal of Applied Mechanics* **58**, pp181-188 (1991).